Force signature of the unzipping transition for strip confined two-dimensional polymers

Aleksander L Owczarek[1] and Andrew Rechnitzer[2]

[1]School of Mathematics and Statistics,
The University of Melbourne, Victoria 3010, Australia.
owczarek@unimelb.edu.au

[2]Department of Mathematics,
University of British Columbia,
Vancouver V6T 1Z2, British Columbia, Canada.
andrewr@math.ubc.ca

August 4, 2017

Abstract

We find and analyse the exact solution of two friendly walks, modelling polymers, confined between two parallel walls in a strip (or slit) where the polymers interact with each other via an attractive contact interaction. In the bulk, where the polymers are always far from any walls, there is an unzipping transition between phases where the two walks drift away for low attractive fugacity (high temperatures) and bind together for high attractive fugacities (low temperatures). Previously this has been used to model the denaturation of DNA. In a strip the transition is not sharp. However, we demonstrate that there is abrupt change in the repulsive force exerted on the walls of the strip that can be calculated exactly. This provides a physical mechanism for denaturation to be seen in a colloidal dispersion.

1 Introduction

There has been a continued interest in models of the adsorption of polymers on a sticky wall, or walls, and related work on models of the pulling, or stretching, of a polymer away from a wall [1, 2, 3, 4, 5, 6, 7, 8, 9, 10]: this has been in part due to the development of the ability in experiments to micro-manipulate single polymers [11, 12, 13]. The modelling of DNA denaturation [14, 15, 16, 17, 18, 19, 20] has also played a part in this interest.

1

Consider a polymer in dilute solution that is attached to a wall at one or at both ends. Moreover, consider a situation where the wall has an attractive contact interaction with the non-attached monomers of the polymer. In such a case there is a second-order phase transition between a high temperature state, where the polymer drifts away from the surface due to entropic repulsion, and a low temperature state, where the polymer stays close to the surface. When the polymer stays close to the surface it is described as *adsorbed*. This is the so-called *adsorption* transition which has been well studied [1, 2, 21, 3, 22] both through exact solutions of directed walk models in two and three dimensions, and through numerical techniques, such as Monte Carlo and analysis of exact enumeration data. If one considers more than one polymer chain and a single sticky wall there has been some exact solution of models of two polymers with different types of contact interaction [23] on the square lattice but also where one includes an interaction between the two polymers [24]. This inter-polymer interaction is a simple attempt at modelling the interaction that may lead to a unzipping transition as in DNA denaturation. Hence, Tabarra *et al.* [24] studied a model where there was a competition between polymer adsorption and polymer unzipping. There has also been a recent study of a model of three polymers interacting with multiple inter-polymer interactions without a surface [25]. This was an attempt at providing a simple model of polymer gelation with fixed polymerisation.

The situation becomes more complex when a polymer is confined between two sticky walls. This situation has been studied by various directed and non-directed lattice walk models [7, 9, 26, 10, 27, 28, 29], in both two and three dimensions. It should be noted that, both for one wall adsorption and two wall models, two and three dimensional system behave in similar ways. Here the phase diagram of two wall models can depend on the relative mesoscopic size of the polymer relative to the width of the slab/strip and the strengths of the interactions on both walls. A motivation for studying this type of system is related to modelling the stabilization of colloidal dispersions by adsorbed polymers (steric stabilization) and the destabilization when the polymer can adsorb on surfaces of different colloidal particles (sensitized flocculation). A polymer confined between two parallel plates exerts a repulsive force on the confining plates because of the loss of configurational entropy unless the polymer is attracted to both walls when it can exert an effective attractive force at large distances. Once again far less is known when one considers multiple polymers confined in this way. A recent exact solution has considered two polymers in two-dimensions where the polymers interact with the two walls via a contact interaction as in the adsorption model [30]. This was motivated by work [28] on ring polymers modelled by self-avoiding polygons, which demonstrate intriguing profiles of the force as a function of Boltzmann weights and strip width.

In this work we will consider two two-dimensional polymers in a strip where the poly-

mers interact via an inter-polymer attraction and calculate exactly the free energy and forces between the walls of the strip for large strip widths. We show that there is a distinct signature to the force profile arising from the bulk unzipping phase transition. This perhaps could be used experimentally to detect the unzipping transition as it occurs near the force minimum.

In Section 2 we define our model in the strip and in the bulk. We then derive the bulk free energy, using the functional equation methodology, in Section 3. We then set up the functional equations in Section 4 and apply the kernel method to obtain a single equation in Section 5 that we analyse for singularities in Section 6. This allows us to analyse the large width asymptotics of the free energy in Section 7 and the force between the walls induced by the polymers in Section 8. Our central finding from our exact results is that there is a signature of the bulk unzipping transition in the force as a function of temperature, which we note is not monotonic for large widths. We provide a brief summary in Section 9 and point to future directions.

2   Model

We consider pairs of directed paths, taking steps $(1, \pm 1)$, of equal total length n in the width w strip of the square lattice — namely $\mathbb{Z} \times \{0, 1, \ldots, w\}$. These paths may touch (ie share edges and vertices) but not cross. We consider those pairs of paths whose initial vertices lie at $(0, 0)$ and $(0, w)$. See Figure 1.
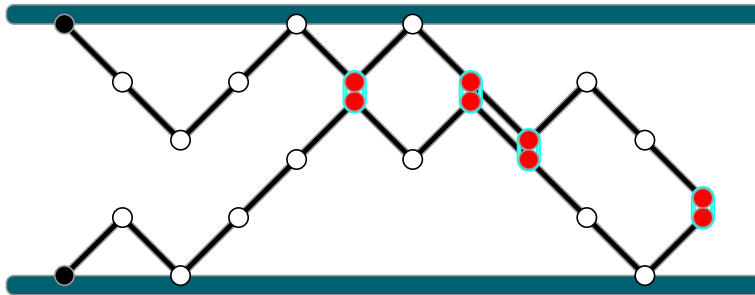

Figure 1: *Two walks confined between two walls spaced w lattice units apart. The walks may share vertices and each shared vertex (contact) contributes a Boltzmann weight c to the partition function. The configuration above will contribute a weight c^4 for length $n = 11$ and width $w = 4$.*

Let $\varphi \in \Omega_n$ be such a pair of paths in the set of fixed length walks Ω_n and define $n = |\varphi|$ to be the length of the paths. If the width of the strip, w, is odd then the paths never share vertices and the combinatorics that follows is more complicated. Because of this we

only consider even widths. Note that this implies that the distance between the endpoints of the paths is always even.

To be specific let φ be a configuration and add the energy $-\varepsilon_c$ for each shared vertex (*contact*) of the two walks. The number of contacts will be denoted $v(\varphi)$. Note that the leftmost vertices being on the walls do not share a vertex as $w \geq 2$. The main model we discuss in the paper is based on pairs of walks, φ, that finish with endpoints together at the same height. Define the corresponding fixed-length partition function to be

$$Z_n(c; w) = \sum_{\varphi \in \Omega_n} e^{\varepsilon_c v(\varphi)/k_B T} = \sum_{\varphi \in \Omega_n} c^{v(\varphi)}, \tag{2.1}$$

where T is the temperature, k_B the Boltzmann constant and $c = e^{\varepsilon_c/k_B T}$ is the Boltzmann weight associated with contacts. The thermodynamic reduced free energy at finite width is given in the usual fashion as

$$\kappa(c; w) = \lim_{n \to \infty} \frac{1}{n} \log \left[Z_n(c; w) \right]. \tag{2.2}$$

Because the model at finite w is essentially one-dimensional, the free energy is an analytic function of c and no thermodynamic phase transitions occur [31]. As noted above, the *infinite strip limit* for the single walk model does display singular behaviour and so we consider the same limit for this model. The *infinite strip free energy* for the two walk model is found analogously by

$$\overline{\overline{\kappa}}(c) = \lim_{w \to \infty} \kappa(c; w) = \lim_{w \to \infty} \lim_{n \to \infty} \frac{1}{n} \log \left[Z_n(c; w) \right]. \tag{2.3}$$

We see that the above quantity may be different when the order of limits is swapped. In fact, if the walks are tethered to different walls then when one takes the width off to infinity first, for any finite walks, the two walks do not see each other: the system is independent of the value of c since no contacts every occur. This *double-half* plane limit is then uninteresting. On the other hand, if one fixes the initial vertices of the two walks at $(0, w/2)$ for both walks then for $w > 2n$ the two walks do not ever see the wall. Hence considering the infinite width limit for such configurations results in the bulk problem without walls.

Let us define the free energy of the bulk problem (*bulk limit*) as

$$\kappa^b(c) = \lim_{n \to \infty} \frac{1}{n} \log Z_n^b(c), \tag{2.4}$$

where $Z_n^b(c)$ is the partition function of the bulk system. The bulk generating function is defined as

$$G^b(c; z) = \sum_{n=0}^{\infty} Z_n^b(c) z^n. \tag{2.5}$$

4

We will calculate the bulk free energy in the next section using the fact that the radius of convergence $z_c^b(c)$ of the generating function $G_b(c; z)$ is related to the free energy as

$$\kappa^b(c) = -\log\left(z_c^b(c)\right). \tag{2.6}$$

Subsequently, once we analyse the finite strip, we shall find that the infinite strip limit is given by this bulk problem so that

$$\kappa^b(c) = \overline{\overline{\kappa}}(c) = \lim_{w \to \infty} \kappa(c; w). \tag{2.7}$$

It should be noted that these two limit need not be the same in other systems [7].

Motivated by the single walk model, we consider the effective force applied to the walls by the polymers

$$\mathcal{F}_n = \frac{1}{2n}\left[\log(Z_n(w)) - \log(Z_n(w-2))\right] \tag{2.8}$$

with a thermodynamic limit of

$$\mathcal{F}(c; w) = \frac{1}{2}\left[\kappa(c; w) - \kappa(c; w-2)\right]. \tag{2.9}$$

Note that since we only consider systems of even width we use the argument $w - 2$ rather than $w - 1$ in this definition.

Given that the double half-plane limit is known from the discussion above, we shall concentrate on the infinite strip limit. In this limit, the free energy does not depend on where the walks end. It turns out that the combinatorics of the model in which the walks end together are easier. Accordingly, we study the generating function

$$G_w(c; z) = \sum_{n=0}^{\infty} Z_n(c; w) z^n, \tag{2.10}$$

where the partition function now counts only those walks which end together. The radius of convergence of the generating function $z_c(c; w)$ is directly related to the free energy via

$$\kappa(c; w) = -\log\left(z_c(c; w)\right). \tag{2.11}$$

3 Solution of system in bulk

Before moving to the full model, we first analyse the model in the bulk without any constraining walls. Consider the pair of walks depicted in Figure 2. This pair of directed walks must start at the same vertex, may share edges of the underlying lattice but they may not cross. We have drawn the two walks as though they have been separated by a

small vertical translation; this was done so as to depict the vertices and edges of each walk clearly. While we are primarily interested in walks whose final vertices coincide, we will actually count the superset of walks whose final vertices may lie at any vertical separation. To this end form the generating function

$$H(r; z, c) = \sum_{\varphi} z^{|\varphi|} c^{v(\varphi)} r^{\ell(\varphi)}, \qquad (3.1)$$

where the sum if over all valid conformations φ, $|\varphi|$ denotes the number of edges in one walk (or equivalently the horizontal span of the conformation), $v(\varphi)$ denotes the number of times the walks coincide at a vertex (excluding the starting vertex) and $\ell(\varphi)$ denotes half the vertical separation of the end vertices (since this vertices are always separated by an even distance). The generating function G is a power series in z with coefficients that are polynomials in r and c. The generating function for the bulk problem we want to calculate $G^b(c; z)$ is given as

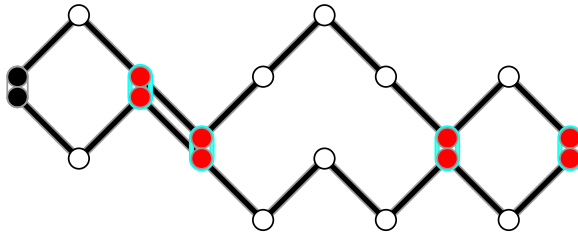$$G^b(c; z) = H(0; z, c). \qquad (3.2)$$

Figure 2: A pair of friendly directed walks in the bulk — these have been drawn after a small vertical translation so as to depict the vertices and edges of each walk clearly. This walk contributes $z^9 c^4 r^0$ to the generating function $H(r; z, c)$.

We now establish a functional equation satisfied by $H(r; z, c)$ via a standard step-by-step construction. A similar construction will be used to derive a functional equation satisfied by the generating function of the full model in a confining strip. Any legal conformation either contains no edges (having horizontal span 0) or can be constructed by appending $\nearrow, \searrow$ edges to the last vertices of each walk (see Figure 3-left).

Translating this to operations on the generating function we obtain

$$H(r) = 1 + z(r + 2 + \bar{r})H(r), \qquad (3.3)$$

where $\bar{r} = 1/r$. However, this counts invalid conformations. In particular (see Figure 3-right), we have constructed paths that cross when appending steps to two walks that end at the same vertex: specifically when adding a $\searrow$ edge to the top walk and a $\nearrow$ edge to
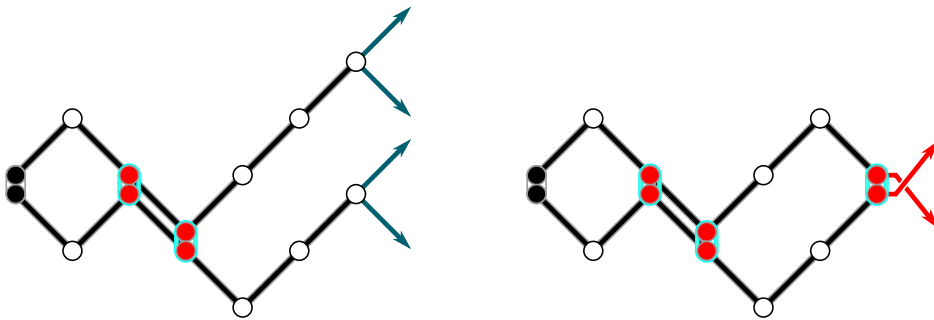
6

Figure 3: (left) Any conformation either contains no edges or can be constructed by appending ↗, ↘ edges to the last vertices of each walk. (right) When we append edges to the end of the walks we must take care to not construct a conformation in which the two paths cross. This occurs precisely when the two walks end together and we append a ↘ to the top walk and a ↗ to the bottom walk.

the bottom walk. These invalid conformations are counted by $z\bar{r}[r^0]H$ and so we subtract this contribution:

$$H(r) = 1 + z(r + 2 + \bar{r})H(r) - z\bar{r}[r^0]H. \tag{3.4}$$

where we have used $[r^k]H$ to denote the coefficient of r^k in $H(r; z, c)$.
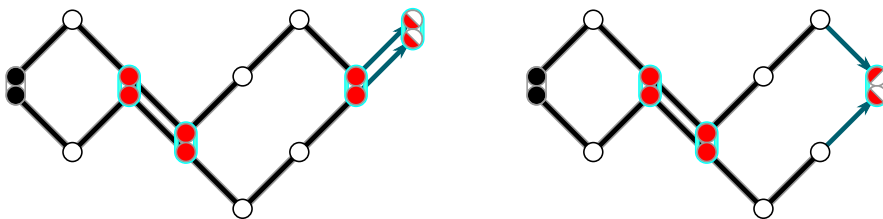

Figure 4: The two figures show how new bound vertex pairs are created in the construction and correspond to the terms in equation (3.5). In both cases, these conformations have already been counted by the construction described in Figure 3 but underweighted by a factor of c. Consequently, we can correct this underweighting by subtracting off the contributions of those conformations and then adding them back with an additional factor of c.

While this construction produces all legal conformations, it does not produce them with the correct weight — we must ensure that walks that end together after appending steps are counted with an additional factor of c. Consider any conformation in which the walks

end together (see Figure 4). This was either obtained by appending a pair of parallel $\nearrow$ or $\searrow$ edges to the end of a conformation in which the walks end together (Figure 4-left) or by appending $\substack{\nearrow \\ \searrow}$ to the ends of walks that are separated by 2 lattice spacings (Figure 4-right). To correct the weight of such conformations we subtract their contributions from the functional equation and then put them back with an additional factor of c. Consequently, they contribute the following terms to the functional equation

$$2z(c-1) \cdot [r^0]H + z(c-1) \cdot [r^1]H. \tag{3.5}$$

Putting everything together we arrive at the full functional equation

$$H(r) = 1 + z(r + 2 + \bar{r})H(r) + z\bar{r} \cdot [r^0]H + 2z(c-1) \cdot [r^0]H + z(c-1) \cdot [r^1]H. \tag{3.6}$$

We can eliminate one of the unknowns from this equation by establishing a relationship between $[r^0]H$ and $[r^1]H$. Extracting the coefficient of r^0 in the equation (3.6):

$$\begin{aligned} [r^0]H &= 1 + 2z[r^0]H + z[r^1]H + 2z(c-1) \cdot [r^0]H + z(c-1) \cdot [r^1]H \\ &= 1 + 2zc[r^0]H + zc[r^1]H. \end{aligned} \tag{3.7}$$

This can also be established by an equivalent combinatorial construction; again examine Figure 4. Every pair of walks that ends together is either a single pair of vertices or is constructed by appending parallel $\nearrow$ or $\searrow$ edges to the end of a pair of walks that end together, or by appending $\substack{\nearrow \\ \searrow}$ edges to a pair of walks that end 2 lattice spacings apart.

Using equation (3.7) we can write $[r^1]H$ in terms of $[r^0]H$ and then substitute that into equation (3.6). Rearranging the result we have

$$K(r) \cdot H(r) = \frac{1}{c} + \left(1 - \frac{1}{c} - \frac{z}{r}\right) \cdot [r^0]H, \tag{3.8}$$

where the kernel, $K(r; z) \equiv K(r)$, is given by

$$K(r) = 1 - z(r + 2 + \bar{r}).$$

We can also arrive at equation (3.8) in an alternative fashion. First rearrange the equation as follows:

$$H(r) + \frac{1}{c}[r^0]H = \frac{1}{c} + z(r + 2 + \bar{r})H(r) - z\bar{r}[r^0]H + [r^0]H. \tag{3.9}$$

The left-hand side of the equation counts all conformations but double-counts those in which walks end together. Those conformations are counted once with their correct weights (by the $H(r)$ term) and then again but with weights reduced by a factor of c (the $\frac{1}{c}[r^0]H$ term). Now split the right-hand side into two parts —the first 3 terms and then the last

8

term. The first 3 terms count all conformations with their correct weights excepting that those in which walks end together are underweighted by a factor of c. The last term then counts conformations in which the walks together with their correct weights. Hence both sides of the equation count the same set of weighted objects.

We solve this equation by setting the kernel to zero by a choice of r. Solving $K(r) = 0$ gives

$$r_+(z) = \frac{1 - 2z + \sqrt{1 - 4z}}{2z} = z^{-1} - 2 - z - 2z^2 + O(z^3) \tag{3.10a}$$

$$r_-(z) = \frac{1 - 2z - \sqrt{1 - 4z}}{2z} = z + 2z^2 + O(z^3). \tag{3.10b}$$

Standard arguments show that $H(r_+(z))$ is not convergent in the space of formal power series, while $H(r_-(z))$ is convergent. Consequently, substituting $r = r_-(z)$ into equation 3.8 gives

$$0 = \frac{1}{c} + \left(1 - \frac{1}{c} - \frac{z}{r_-(r)}\right) \cdot [r^0]H, \tag{3.11}$$

which rearranges to give us the required generating function:

$$G^b(c; z) = [r^0]H = \frac{2 - c - 2zc - c\sqrt{1 - 4z}}{2(c^2 z^2 + 2(c - 1)cz - c + 1)}. \tag{3.12}$$

The full $H(r; z, c)$ generating function can also be found (if needed) by substituting this back into equation (3.8).

From this solution we can find the dominant singularity:

$$z_c^b(c) = \begin{cases} \frac{1}{4} & c \le 4/3 \\ \frac{1 - c + \sqrt{c^2 - c}}{c} & c \ge 4/3 \end{cases} \tag{3.13}$$

and so the bulk free energy, $\kappa^b(c) = -\log z_c^b(c)$. This is plotted in Figure 5.

Notice that the form of the dominant singularity changes at $c = 4/3$ and that this change indicates a phase transition from an unzipped regime with few contacts to a zipped regime with a positive density of contacts. We can compute the density of contacts by taking the log-derivative of the dominant singularity, or we can obtain more detailed asymptotics using (now standard) analytic combinatorics methods (see [32]). These give

$$\text{mean number of contacts} = \begin{cases} \frac{3c+4}{4-3c} + O(n^{-1}) & c < 4/3 \\ \frac{3\sqrt{\pi}}{2} \cdot \sqrt{n} + O(1) & c = 4/3 \\ \frac{c - 2 + \sqrt{c(c-1)}}{2(c-1)} \cdot n + O(1) & c > 4/3. \end{cases} \tag{3.14}$$
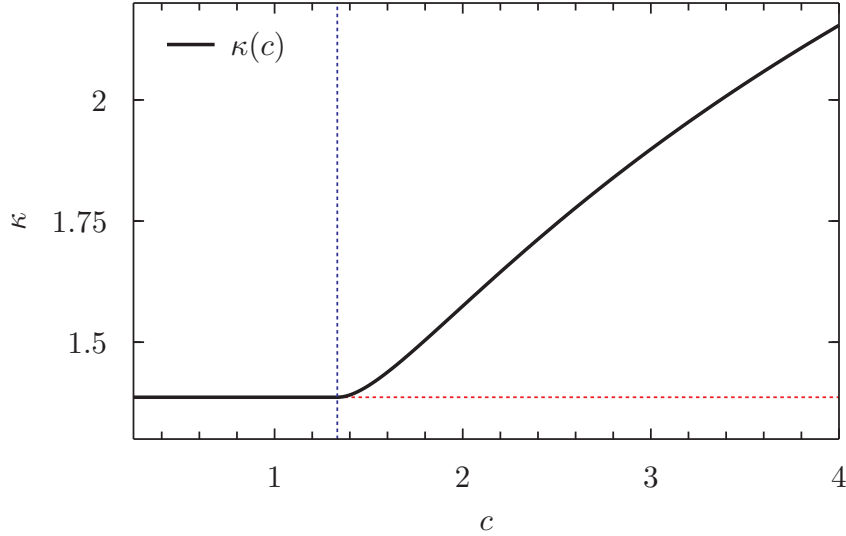
9

Figure 5: The free energy of the system in the bulk as a function of the zipping interaction c. We have indicated the location of the phase transition at $c = 4/3$ with the blue vertical dashed line. The red horizontal dashed line indicates the free energy of the system at small c, namely $\kappa = \log 4$.

We note here that the transformation

$$c \mapsto \frac{(d+1)^2}{2d+1} \tag{3.15}$$

rationalises the radius of convergence:

$$z_c^b(d) = \begin{cases} \frac{1}{4} & d \leq 1 \\ \frac{d}{(1+d)^2} & d \geq 1. \end{cases} \tag{3.16}$$

We will make use of this transformation when we study the large-c asymptotic behaviour of the full model.

4 The functional equation of the model in a strip

In this section we derive the functional equation satisfied by the generating function of the full model. This is very similar to that of the previous section excepting that we now have to take into account the possibility that in appending steps to the end of the walks that we might produce a confirmation that escapes from the bounding walls. Form the generating function

$$F_w(r, s; z, c) = \sum_{\varphi} z^{|\varphi|} c^{v(\varphi)} r^{\perp(\varphi)} s^{\top(\varphi)}, \tag{4.1}$$

where, as before, z and c are conjugate to the horizontal span and the number of shared vertices respectively, while $\perp(\varphi)$ denotes the distance between the bottom wall and the last vertex of the bottom walk. Similarly, $\top(\varphi)$ denotes the distance between the top wall and the final vertex of the top walk. Note that, where the context is clear, we will also write $F_w(r, s; z, c) \equiv F_w(r, s) \equiv F(r, s)$. Once again the generating function of interest occurs when our extra variables are set to zero:

$$G_w(c; z) = F_w(0, 0; z, c). \tag{4.2}$$

By grouping coefficients of r and s together we can write $F(r, s)$ as

$$F(r, s) = \sum_{0 \le i, j \le w} f_{i,j}(z; c) r^i s^j. \tag{4.3}$$

This in turn allows us to express a number of auxillary functions that we require to state the functional equation satisfied by $F(r, s)$:

$$[r^i s^j] F = f_{i,j}(z; c) \tag{4.4a}$$

$$[r^i] F = \sum_j f_{i,j}(z; c) s^j \tag{4.4b}$$

$$[s^j] F = \sum_i f_{i,j}(z; c) r^i \tag{4.4c}$$

$$F_d(x) = \sum_{i=0}^{w} f_{i,w-i}(z; c) x^i \tag{4.4d}$$

$$F_n(x) = \sum_{i=0}^{w} f_{i,w-i-2}(z; c) x^i. \tag{4.4e}$$

The generating function $[r^i s^j] F(r, s)$ counts walks whose final vertices lie at a vertical distance i, j (respectively) from the walls, while F_d counts walks that end on the same vertex and F_n counts walks that end 2 units apart. Notice that $F_d(x)$ and $F_n(x)$ play much the same role as $[r^0] H$ and $[r^1] H$ did in the bulk system.

In this system any conformation either has horizontal span 0, or can be constructed by appending $\nearrow, \searrow$ steps to the end of each walk (see Figure 6). This leads to

$$F(r, s) = 1 + z(r + \bar{r})(s + \bar{s}) F(r, s). \tag{4.5}$$

Notice that this bulk term is different from that of the previous section because the auxiliary variables are conjugate to the distance from each wall rather than the distance between the endpoints. In appending edges to the ends of the walk in this way we will produce invalid conformations — some will will escape from the confining walls while others will produce walks that cross. Walks can escape in 3 different ways: the lower walk escapes
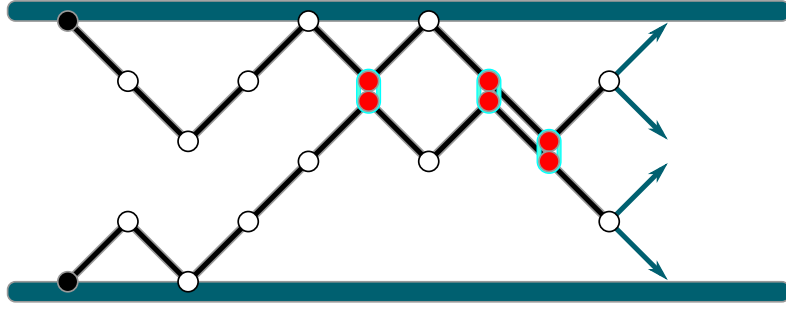
Figure 6: Any conformation either contains no edges or can be constructed by appending $\nearrow, \searrow$ edges to the last vertices of each walk.

over the bottom wall, the upper walk escapes over the top wall, or the walks escape over opposite walls at the same time. Notice that the case of both walks escaping together over the same wall will be counted by one of the first two cases.
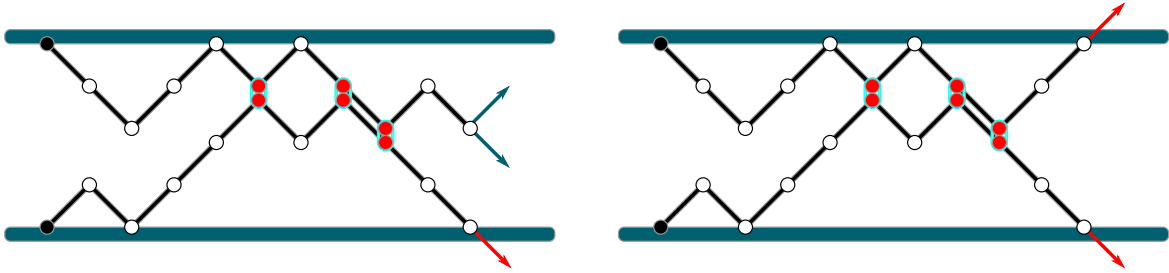

Figure 7: (left) An invalid conformation is generated when a $\searrow$ step is appended to a conformation in which the bottom walk ends on the bottom wall. A similarly invalid conformation will be generated when a $\nearrow$ step is appended to a conformation in which the top walk ends on the top wall. (right) An invalid conformation is generated when a $\searrow$ and $\nearrow$ are (respectively) appended to a conformation in which each walk ends on opposite walls. This conformation is actually a special case of that illustrated on the left.

See Figure 7-left. Conformations in which the bottom walk ends on the bottom wall are counted by $[r^0]F$, and so invalid conformations in which the bottom walk escapes over the bottom wall are counted by

$$z\bar{r}(s + \bar{s})[r^0]F. \tag{4.6a}$$

Similarly, invalid conformations in which the top walk escapes over the top wall are counted by

$$z\bar{s}(r + \bar{r})[s^0]F. \tag{4.6b}$$

Finally invalid conformations in which the walks escape over opposite walls at the same time (see Figure 7-right) are counted by

$$z\bar{r}\bar{s}[r^0s^0]F. \tag{4.6c}$$

Care must be taken not to double-count these invalid conformations. The conformations counted by (4.6c) are counted by both (4.6a) and (4.6b). Hence we must subtract off (4.6a) and (4.6b) from equation 4.5 and then add back (4.6c).
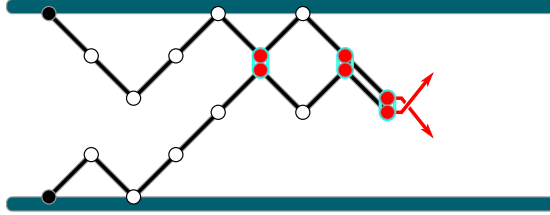

Figure 8: An invalid conformation in which the walks cross is generated by appending a ↗ step to the bottom walk and a ↘ step to the top walk in a conformation in which the walks end together.

We must also remove conformations in which the walks cross. These are generated by appending steps to walks that end together (see Figure 8). These invalid conformations are counted by

$$zrs^{w+1}F_d(r/s). \tag{4.6d}$$

To see this note that $s^wF_d(r/s)$ counts all conformations in which both walks end together, and appending a ↗ step to the lower walk increases the weight by a factor of r, while appending a ↘ step to the top walk increases the weight by a factor of s. Putting these contributions we arrive at the (still incomplete) functional equation

$$\begin{aligned} F(r,s) &= 1 + z(r+\bar{r})(s+\bar{s})F(r,s) \\ &\quad - z\bar{s}(r+\bar{r})F(r,0) - z\bar{r}(s+\bar{s})F(0,s) + z\bar{r}\bar{s}F(0,0) - zrs^{w+1}F_d(r/s). \end{aligned} \tag{4.7}$$

To complete the equation we must correctly weight new shared vertices. See Figure 9. Such vertices occur in two ways (just as was the case in the analysis of walks in the bulk in the previous section) — either a parallel pair of edges is added to a conformation in which the walks end together or by appending ⤢ edges to the ends of walks that are separated by 2 lattice spacings. As was the case in the previous section, these conformations have already been counted but with the wrong weight. Hence we must subtract off their contributions and add them back with an additional factor of c:

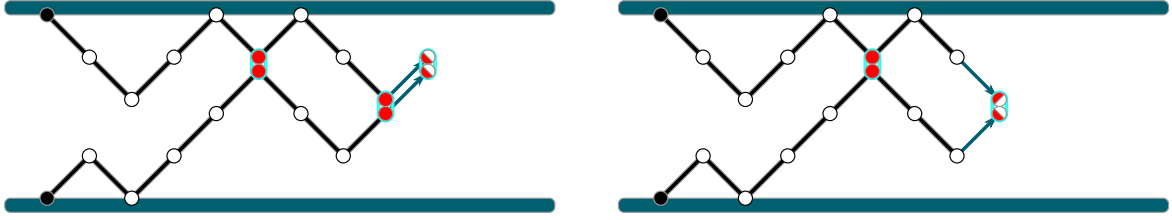$$z(c-1)(r\bar{s} + s\bar{r})s^wF_d(r/s) + z(c-1)s^wF_n(r/s). \tag{4.8a}$$

Figure 9: A new shared vertex is created by either appending a pair of parallel edges to a pair of walks that ends together (left) or by appending appending ⤢ edges to the ends of walks that are separated by 2 lattice spacings.

Unfortunately, the first of these two cases may generate conformations in which the walks escape over one of the walls (see Figure 10) and so we must subtract off those contributions. Such walks are counted by

$$z(c-1)\bar{r}s^{w+1}[r^0 s^w]F + z(c-1)r^{w+1}\bar{s}[r^w s^0]F. \tag{4.8b}$$

The first of these terms counts walks stepping over the bottom wall, while the latter counts those escaping over the top wall.
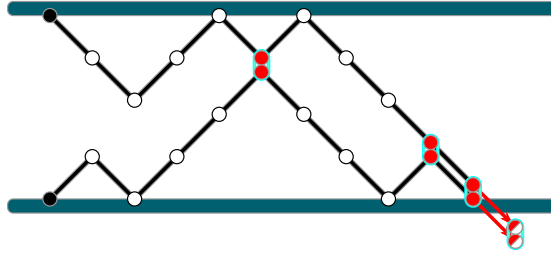

Figure 10: When adding parallel edges and a shared vertex, we must be careful not to construct a new conformation that steps over either wall.

Putting all of these contributions together we arrive at the full functional equation

$$\begin{aligned}
F(r,s) = 1 &+ z(r+\bar{r})(s+\bar{s})F(r,s) \\
&- z\bar{s}(r+\bar{r})F(r,0) - z\bar{r}(s+\bar{s})F(0,s) + z\bar{r}\bar{s}F(0,0) - zrs^{w+1}F_d(r/s) \\
&+ z(c-1)(r\bar{s}+s\bar{r})s^W F_d(r/s) + z(c-1)s^w F_n(r/s) \\
&- z(c-1)r^{w+1}\bar{s}\cdot[r^w s^0]F(r,s) - z(c-1)s^{w+1}\bar{r}\cdot[r^0 s^w]F(r,s).
\end{aligned} \tag{4.9}$$

We can eliminate two unknowns from the system by establishing the following relationships

$$[r^w s^0]F = [r^0 s^w]F \tag{4.10a}$$

$$\begin{aligned}
s^w F_d(r/s) = z(r\bar{s}+s\bar{r})cs^w F_d(r/s) &+ zcs^w F_n(r/s) \\
&- zc(s^{w+1}\bar{r}\cdot[r^0 s^w]F + r^{w+1}\bar{s}\cdot[r^w s^0]F).
\end{aligned} \tag{4.10b}$$

14

The first of these follows from the vertical symmetry of the model. The second can be obtained by considering the "diagonal" coefficients of equation (4.9) — ie computing $\sum_{i=0}^{w}[r^i s^{w-i}]$ of both sides:

$$
\begin{aligned}
s^w F_d(r/s) = {}& 0 + z(r\bar{s} + s\bar{r})s^w F_d(r/s) + zs^w F_n(r/s) \\
& - zr^{w+1}\bar{s}[r^w s^0]F - z\bar{r}s^{w+1}[r^0 s^w]F + 0 - 0 \\
& + z(c-1)(r\bar{s} + s\bar{r})s^W F_d(r/s) + z(c-1)s^w F_n(r/s) \\
& - z(c-1)r^{w+1}\bar{s}\cdot[r^w s^0]F(r,s) - z(c-1)s^{w+1}\bar{r}\cdot[r^0 s^w]F(r,s).
\end{aligned}
\tag{4.11}
$$

Collecting like terms in the above gives (4.10b). One can also establish the same equation combinatorially by considering all the ways in which one can produce a conformation in which the walks end at the same vertex. See Figure 9. Any pair of walks that end at the same vertex can be obtained by either appending parallel edges to the end of a walk counted by F_d or by appending $\nearrow\!\!\!\nwarrow$ edges to the ends of a walk counted by F_n. However, in so doing, one constructs walks that escape over the top or bottom wall (see Figure 10).

We can now eliminate $[r^w s_0]F$ and $F_n(r/s)$ by solving equations (4.10a) and (4.10b) for those terms and substituting them back into (4.9). Cleaning up the result gives us

$$
\begin{aligned}
K(r,s)\cdot F(r,s) = {}& 1 - z\bar{s}(r+\bar{r})F(r,0) - z\bar{r}(s+\bar{s})F(0,s) + z\bar{r}\bar{s}F(0,0) \\
& + \left(1 - \frac{1}{c} - zrs\right)s^w F_d(r/s),
\end{aligned}
\tag{4.12}
$$

where K is the kernel of the equation and is given by

$$
K = 1 - z(r+\bar{r})(s+\bar{s}).
\tag{4.13}
$$

In the next section we will use symmetries of the kernel to remove more unknowns from this functional equation.

Notice that by rearranging the equation as follows

$$
\begin{aligned}
F(r,s) + \frac{1}{c}\cdot s^W F_d(r/s) = {}& 1 + z(r+\bar{r})(s+\bar{s})F(r,s) \\
& - z\bar{s}(r+\bar{r})F(r,0) - z\bar{r}(s+\bar{s})F(0,s) + z\bar{r}\bar{s}F(0,0) \\
& - zrs^{w+1}F_d(r/s) \\
& + s^w F_d(r/s),
\end{aligned}
\tag{4.14}
$$

we can interpret it combinatorially in an analogous way as we did for the bulk case. The left-hand side counts all walks but also double-counts walks which end together — one copy has the correct weight, while another copy is underweighted by a factor of c. The right-hand side counts the same set of walks — the terms on the first 3 lines construct all valid conformations, but any walks that finish together are underweighted by a factor of c. The last line then adds back in walks which finish together but with the correct weight. Hence both sides count the same set of conformations with the correct weights.

15

5 The kernel method

Consider again the full functional equation (4.12) and its kernel (4.13):

$$K(r,s) \cdot F(r,s) = 1 - z\bar{s}(r+\bar{r})F(r,0) - z\bar{r}(s+\bar{s})F(0,s) + z\bar{r}\bar{s}F(0,0)$$

$$+ \left(1 - \frac{1}{c} - zrs\right)s^w F_d(r/s) \tag{5.1}$$

$$K(r,s) = 1 - z(r+\bar{r})(s+\bar{s}). $$

This is a single equation in 5 unknown (but related) functions. We will remove some of these unknowns by taking advantage of symmetries of the kernel — this approach is frequently referred to as the kernel method [33] and shares many similarities with the classical method of images. The approach we describe below is very similar to that used in [34, 30].

Notice that the kernel is invariant under the involutions

$$r \mapsto \bar{r} \qquad\qquad \text{and} \qquad\qquad s \mapsto \bar{s} \tag{5.2}$$

Using this we construct three new equations by setting $(r,s) \mapsto (\bar{r},s), (r,\bar{s}), (\bar{r},\bar{s})$:

$$K(r,s) \cdot F(\bar{r},s) = 1 - z\bar{s}(r+\bar{r})F(\bar{r},0) - zr(s+\bar{s})F(0,s) + zr\bar{s}F(0,0)$$

$$+ \left(1 - \frac{1}{c} - z\bar{r}s\right)s^w F_d(1/rs), \tag{5.3a}$$

$$K(r,s) \cdot F(r,\bar{s}) = 1 - zs(r+\bar{r})F(r,0) - z\bar{r}(s+\bar{s})F(0,\bar{s}) + z\bar{r}sF(0,0)$$

$$+ \left(1 - \frac{1}{c} - zr\bar{s}\right)s^{-w} F_d(rs), \tag{5.3b}$$

$$K(r,s) \cdot F(\bar{r},\bar{s}) = 1 - zs(r+\bar{r})F(\bar{r},0) - zr(s+\bar{s})F(0,\bar{s}) + zrsF(0,0)$$

$$+ \left(1 - \frac{1}{c} - z\bar{r}\bar{s}\right)s^{-w} F_d(s/r). \tag{5.3c}$$

In so doing we have introduced more unknowns, but we can eliminate several of these by taking appropriate linear combinations of the original functional equation and these 3 new equations:

$$c \cdot K(r,s)\left[rsF(r,s) - \bar{r}sF(\bar{r},s) - r\bar{s}F(r,\bar{s}) + \bar{r}\bar{s}F(\bar{r},\bar{s})\right] = c(s-\bar{s})(r-\bar{r})$$

$$- (crsz - c + 1)rs^{w+1}F_d(r/s) - (cz - crs + rs)r^{-2}s^{-2-w}F_d(s/r)$$

$$+ (crz - cs + s)rs^{-2-w}F_d(rs) + (csz - cr + r)r^{-2}s^{1+w}F_d(1/rs). \tag{5.4}$$

This combination eliminates the unknowns $F(r,0), F(\bar{r},0), F(0,s), F(0,\bar{s}), F(0,0)$.

We can eliminate two more unknowns by again taking advantage of the vertical symmetry of the system and noting that

$$F_d(s/r) = (s/r)^w F_d(r/s) \qquad \text{and} \qquad F_d(1/rs) = (rs)^{-w} F_d(rs). \tag{5.5}$$

This gives us

$$c \cdot K(r,s)\left[rsF(r,s) - \bar{r}sF(\bar{r},s) - r\bar{s}F(r,\bar{s}) + \bar{r}\bar{s}F(\bar{r},\bar{s})\right] = c(s-\bar{s})(r-\bar{r})$$
$$- \left[(crsz - c + 1)rs^{w+1} + (cz - crs + rs)r^{-2-w}s^{-2}\right]F_d(r/s)$$
$$+ \left[(crz - cs + s)rs^{-2-w} + (csz - cr + r)r^{-2-w}s\right]F_d(rs). \quad (5.6)$$

We can now remove the unknowns from the left-hand side of this equation by choosing values of r, s that set the kernel equal to zero, providing that the functions $F(r,s), F(\bar{r},s), F(r,\bar{s})$ and $F(\bar{r},\bar{s})$ all converge at those choices.

Now let $\hat{r}, \hat{s}$ be a solution of $K(r,s) = 0$, and in general $\hat{r}, \hat{s}$ will be Laurent series in z. Notice that the series $F(\hat{r}, \hat{s})$ will be well defined because the coefficient of z^n in $F(r,s)$ is a polynomial of degree at most w in both r and s. Similarly the series $F(1/\hat{r}, \hat{s}), F(\hat{r}, 1/\hat{s}), F(1/\hat{r}, 1/\hat{s})$ are all well defined and converge in the space of formal power series. Substituting $(r,s) \mapsto (\hat{r}, \hat{s})$ into equation (5.6) then eliminates all but two unknowns from the functional equation:

$$0 = c(\hat{s} - \bar{\hat{s}})(\hat{r} - \bar{\hat{r}})$$
$$- \left[(c\hat{r}\hat{s}z - c + 1)\hat{r}\hat{s}^{w+1} + (cz - c\hat{r}\hat{s} + \hat{r}\hat{s})\hat{r}^{-2-w}\hat{s}^{-2}\right]F_d(\hat{r}/\hat{s}) \quad (5.7)$$
$$+ \left[(c\hat{r}z - c\hat{s} + \hat{s})\hat{r}\hat{s}^{-2-w} + (c\hat{s}z - c\hat{r} + \hat{r})\hat{r}^{-2-w}\hat{s}\right]F_d(\hat{r}\hat{s}).$$

At this point it makes sense to make a change of variables

$$rs \mapsto p \qquad \text{and} \qquad r/s \mapsto q \qquad (5.8)$$

with corresponding kernel solutions

$$\hat{r}\hat{s} \mapsto \hat{p} \qquad \text{and} \qquad \hat{r}/\hat{s} \mapsto \hat{q} \qquad (5.9)$$

This maps the original kernel to a new kernel

$$\hat{K}(p,q) = 1 - z\frac{(p+q)(1+pq)}{pq}. \qquad (5.10)$$

Changing variables in this way gives us the equation

$$0 = c\hat{p}^{w/2-1}\hat{q}^{w/2-1}(\hat{p}\hat{q} - 1)(\hat{p} - \hat{q}) + \left[(c\hat{q}z - c + 1)\hat{q}^{w+1} + (cz - c\hat{q} + \hat{q})\hat{q}^{-2}\right]F_d(\hat{p})$$
$$- \left[(c\hat{p}z - c + 1)\hat{p}^{w+1} + (cz - c\hat{p} + \hat{p})\hat{p}^{-2}\right]F_d(\hat{q}). \quad (5.11)$$

Now using the kernel $\hat{K}$ we can also eliminate z from this expression by noting that

$$z = \frac{\hat{p}\hat{q}}{(\hat{p} + \hat{q})(1 + \hat{p}\hat{q})}. \qquad (5.12)$$

This finally gives us (after clearing denominators) the equation

$$0 = c\hat{p}^{w/2}\hat{q}^{w/2}(\hat{p}\hat{q} - 1)(\hat{p} - \hat{q})(\hat{q} + \hat{p})(\hat{p}\hat{q} + 1)$$
$$+ \left[(c\hat{p}\hat{q}^2 - \hat{p}^2\hat{q} - \hat{p}\hat{q}^2 + c\hat{p} + c\hat{q} - \hat{p} - \hat{q})\hat{p}^{w+2}\hat{q} + (c\hat{p}^2\hat{q} + c\hat{p}\hat{q}^2 - \hat{p}^2\hat{q} - \hat{p}\hat{q}^2 + c\hat{p} - \hat{p} - \hat{q})\hat{q}\right]F_d(\hat{q})$$
$$- \left[(c\hat{p}^2\hat{q} - \hat{p}^2\hat{q} - \hat{p}\hat{q}^2 + c\hat{p} + c\hat{q} - \hat{p} - \hat{q})\hat{p}\hat{q}^{w+2} + (c\hat{p}^2\hat{q} + c\hat{p}\hat{q}^2 - \hat{p}^2\hat{q} - \hat{p}\hat{q}^2 + c\hat{q} - \hat{p} - \hat{q})\hat{p}\right]F_d(\hat{p}).$$
$$(5.13)$$

6   Finding singularities

We adapt the method from [34] to establish the locations of the singularities of the function F_d. Let us first do this when $c = 1$ to demonstrate the idea of the method. In this case the functional equation simplifies considerably to

$$0 = \hat{p}^{w/2}\hat{q}^{w/2}(\hat{p}\hat{q} - 1)(\hat{p} - \hat{q})(\hat{q} + \hat{p})(\hat{p}\hat{q} + 1) + \left[\hat{p}^{w+4} + 1\right]\hat{q}^2 F_d(\hat{q}) + \left[\hat{q}^{w+4} + 1\right]\hat{p}^2 F_d(\hat{p}).$$
$$(6.1)$$

Now choose $\hat{p}$ so that the coefficient of $F_d(\hat{q})$ is zero — that is $\hat{p}^{w+4} = -1$ — call this value p_*. This eliminates $F_d(\hat{q})$ from the equation and we can isolate $F_d(p_*)$ as

$$F_d(p_*) = \frac{p_*^{w/2-2}\hat{q}^{w/2}(p_*\hat{q} - 1)(p_* - \hat{q})(\hat{q} + p_*)(p_*\hat{q} + 1)}{\hat{q}^{w+4} + 1}.$$
$$(6.2)$$

The function $F_d(p_*)$ is a rational function of z and so has simple poles. The only sources of such singularities in the above expression come from the zeros of the denominator, that is when $\hat{q}^{w+4} + 1 = 0$. Hence singularites $z(p, q)$ satisfy

$$\hat{p}^{w+1} + 1 = 0 \quad \text{and} \quad \hat{q}^{w+4} + 1 = 0 \quad \text{with} \quad (p\hat{q} - 1)(p - \hat{q})(\hat{q} + p)(p\hat{q} + 1) \neq 0. \quad (6.3)$$

More generally when $c \neq 1$ we have an expression of the form

$$X(\hat{p}, \hat{q}) + Y(\hat{p}, \hat{q})F_d(\hat{p}) + Z(\hat{p}, \hat{q})F_d(\hat{q}) = 0. \quad (6.4)$$

Now if $Y(\hat{p}, \hat{q}) = 0$ by some choice of $\hat{p} = \hat{p}_*$ then since (z, p, q) satisfy two polynomial equations, we can consider both $\hat{p}_*, \hat{q}_*$ as functions of z and write

$$F_d(\hat{p}_*) = -\frac{X(\hat{p}_*, \hat{q}_*)}{Z(\hat{p}_*, \hat{q}_*)}. \quad (6.5)$$

The simple poles of F_d now come from the zeros of $Z(\hat{p}_*\hat{q}_*)$. Hence singularities $z(p, q)$ satisfy

$$Y(p, q) = 0 \qquad \text{and} \qquad Z(p, q) = 0 \qquad \text{with} \qquad X(p, q) \neq 0. \qquad (6.6)$$

18

Substituting in Y, Z we get

$$\hat{p}^{w+4} = -\frac{(C\hat{p}^2\hat{q} + C\hat{p}\hat{q}^2 + C\hat{p} - \hat{q})}{(C\hat{p}\hat{q}^2 - \hat{p}^2\hat{q} + C\hat{p} + C\hat{q})}, \tag{6.7a}$$

$$\hat{q}^{w+4} = -\frac{(C\hat{p}^2\hat{q} + C\hat{p}\hat{q}^2 + C\hat{q} - \hat{p})}{(C\hat{p}^2\hat{q} - \hat{p}\hat{q}^2 + C\hat{p} + C\hat{q})}, \tag{6.7b}$$

$$0 \neq (\hat{p}\hat{q} - 1)(\hat{p} - \hat{q})(\hat{q} + \hat{p})(\hat{p}\hat{q} + 1). \tag{6.7c}$$

We have been unable to solve these equations in closed form except at $c = 1$. In the next section we derive asymptotic expressions for the solutions when w is large.

7 Asymptotics of free energy

In order to determine the asymptotic solutions of the zero equations (6.7), we first solved them numerically for small w at various values of c — see Figure 11. Notice that all the
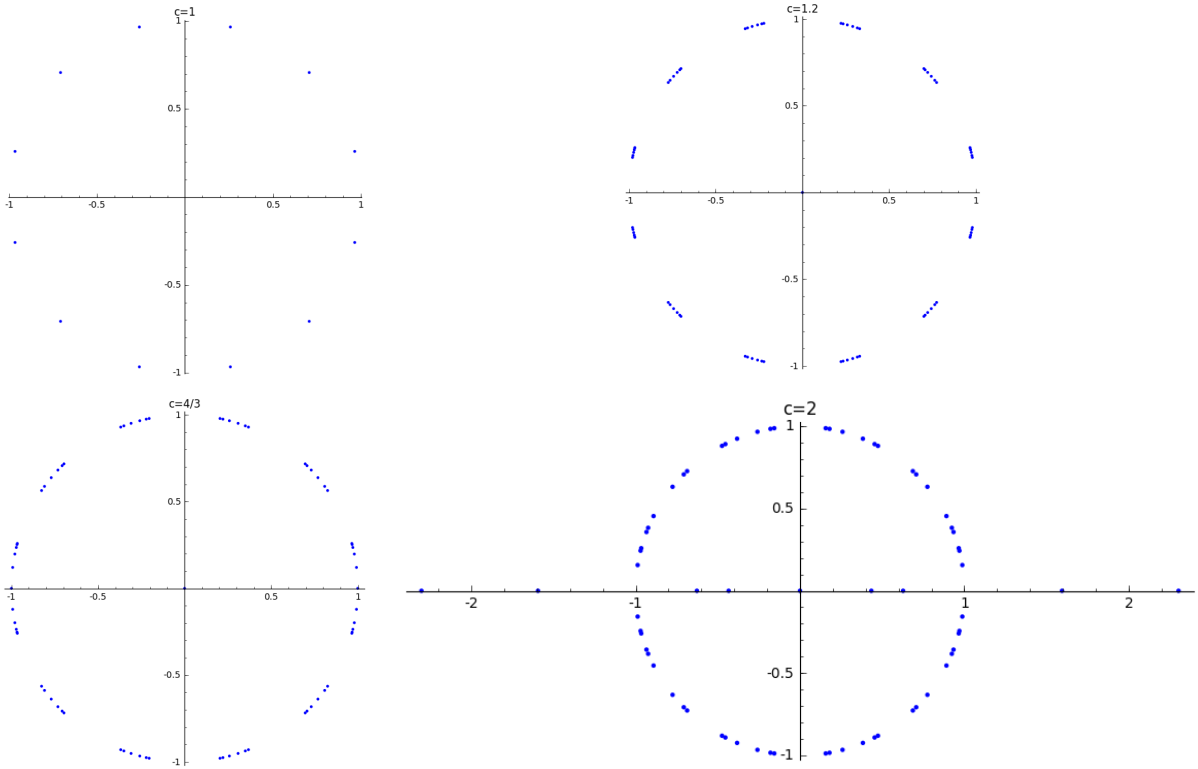

Figure 11: A plot of the $\hat{p}$-zeros of equations (6.7) for $w = 8$ and $c = 1, 6/5, 4/3, 2$ (top-left, top-right, bottom-left, bottom-right respectively).

zeros lie on the unit circle for $c \leq 4/3$ and either on the unit circle or the real line for $c > 4/3$. Because of this we consider the three regimes — $c < 4/3$, $c = 4/3$ and $c > 4/3$ —

in turn: recall from the bulk solution in section 3 that these parameter regimes corespond to the unzipped, critical and zipped phases respectively.

7.1 Unzipped regime — $c < 4/3$

As noted above, when $c = 1$ the system reduces to the uncoupled equations

$$\hat{p}^{w+4} = -1 \qquad\qquad \hat{q}^{w+4} = -1. \tag{7.1}$$

Hence both are $(w+4)^{\text{th}}$ roots of -1:

$$\hat{p} = \exp\left(\pi i \frac{j}{w+4}\right) \qquad\qquad \hat{q} = \exp\left(\pi i \frac{k}{w+4}\right). \tag{7.2}$$

with j, k odd integers. Hence

$$z = \frac{1}{2} \cdot \frac{1}{\cos(\pi j/(w+4)) + \cos(\pi k/(w+4))}. \tag{7.3}$$

The dominant singularity should come from j, k chosen as small as possible. This suggests $j = k = 1$, however this gives $\hat{p} = \hat{q}$ which violates equation (6.7c). Hence the smallest possible choice is $j = 1, k = 3$ or vice-versa. With this choice we obtain

$$z_c(1) = \frac{1}{2} \cdot \frac{1}{\cos(\pi/(w+4)) + \cos(3\pi/(w+4))} \tag{7.4}$$

$$= \frac{1}{4} \cdot \frac{1}{\cos(\pi/(w+4))\cos(2\pi/(w+4))} \tag{7.5}$$

$$\sim \frac{1}{4} + \frac{5\pi}{8} w^{-2} - 5\pi w^{-3} + \cdots, \tag{7.6}$$

which recovers the comparable result in [30].

We can then perturb around this solution by looking for (asymptotic) solutions of the form

$$\hat{p}, \hat{q} = \exp\left(\frac{i\pi}{w+4} \cdot \sum_j x_j w^{-j}\right). \tag{7.7}$$

This leads to

$$\hat{p} = \exp\left(\frac{\pi}{w+4} \cdot \left(1 + \frac{8(c-1)}{3c-4} w^{-1} - \frac{32(c-1)(c-2)}{(3c-4)^2} w^{-2}, + \cdots\right)\right) \tag{7.8a}$$

$$\hat{q} = \exp\left(\frac{3\pi}{w+4} \cdot \left(1 + \frac{24(c-1)}{3c-4} w^{-1} - \frac{96(c-1)(c-2)}{(3c-4)^2}, w^{-2} + \cdots\right)\right) \tag{7.8b}$$

and so

$$z_c(c) = \frac{1}{4} + \frac{5\pi^2}{8} w^{-2} - \frac{5\pi^2(c-2)}{(3c-4)} w^{-3} + \cdots. \tag{7.9}$$

Notice this recovers the desired asymptotics when $c \to 1$. It is clearly divergent as c approaches $4/3$ and does not apply for $c > 4/3$. We have also verified this form by computing $z_c(c)$ numerically for small w and fixed c by transfer matrix.

7.2 Transition point — $c = 4/3$

Applying the same ansatz when $c = 4/3$ gives asymptotics for $z_c(c)$ which are contradicted by numerical transfer matrix data. Consequently, we examined the solutions of (6.7) in detail for $c = 4/3$ and a range of w-values. More precisely we fixed w at some small number and then computed the resultant to obtain a polynomial equation in p. We found all solutions and verified that they lay on the unit circle. Next we took pairs of solutions (since the system is symmetric in p, q) and computed z via the kernel. Of course, most of these z values correspond to subdominant singularities, but we were able to identify certain p, q pairs that give the dominant singularity as computed via a transfer matrix.

The (p, q) pair corresponding to the dominant singularity lay on the unit circle, but the argument of that p (without loss of generality) decayed as $w^{-3/2}$ rather than w^{-1}. This suggests the more general ansatz

$$\hat{p}, \hat{q} = \exp\left(2i\pi \cdot \sum_j x_j w^{-j/2}\right).$$

With this we find that

$$\hat{p} = \exp\left(i\frac{\pi}{\sqrt{2}}\left(w^{-3/2} - \frac{\pi^2 + 45}{12}w^{-5/2} + \frac{11\pi^4 + 690\pi^2 + 17235}{1140}w^{-7/2} + \cdots\right)\right)$$

$$\hat{q} = \exp\left(2i\pi\left(w^{-1} - \frac{5}{2}w^{-2} + \frac{13}{2}w^{-3} - \frac{\pi^2 + 105}{6}w^{-4} + \cdots\right)\right),$$

which gives

$$z_c(4/3) = \frac{1}{4} + \frac{\pi^2}{4}w^{-2} - \frac{9\pi^2}{8}w^{-3} + \frac{\pi^2(7\pi^2 + 186)}{48}w^{-4} + \cdots.$$

Notice that if we apply this same ansatz for $c < 4/3$ then we recover equation (7.8).

7.3 Zipped regime — $c > 4/3$

Consider the bottom-right plot in Figure 11 corresponding to large c. For $c > 4/3$ we observe that some of the roots of equation (6.7) lie on the real axis. Consequently, we repeat a similar analysis of the zeros, comparing them against the dominant singularity computed by transfer matrix. This showed that the (p, q) pair corresponding to the dominant singularity had (without loss of generality) its p-value on the real line and the q-value on the unit circle. The position of the p-value was asymptotic to a constant plus a term that decayed as w^{-1} and the argument of the q-value decayed as w^{-1}.

Before we go further, notice that as $w \to \infty$ we expect to recover the free energy of the bulk system:

$$\lim_{w\to\infty} z_c = \frac{d}{(1+d)^2}, \tag{7.10}$$

where we have used the rationalising transformation

$$c \mapsto \frac{(d+1)^2}{2d+1}, \tag{7.11}$$

for $c > 4/3$ and $d > 1$. This suggests that $p \to \frac{1}{d}$ and $q \to 1$ as $w \to \infty$ which is also suggested by the numerical work described above. If one sets $p = \frac{1}{d}$ and $q = 1$ in the kernel then one recovers this value of z. This suggests the following ansatz

$$\hat{p} = \frac{1}{d} \sum_j x_j w^{-j}, \tag{7.12}$$

$$\hat{q} = \exp\left(2\pi i \sum_j y_j w^{-j} \right). \tag{7.13}$$

More care must be taken when fitting the asymptotic form because the term p^w is now *exponentially* smaller than all other terms. Thus to leading *polynomial* order in w we solve the equations

$$0 = \frac{d^2 \hat{p}^2 \hat{q} + d^2 \hat{p} \hat{q}^2 + d^2 \hat{p} - 2d\hat{q} - \hat{q}}{d^2 \hat{p} \hat{q}^2 - 2d\hat{p}^2 \hat{q} + d^2 \hat{p} + d^2 \hat{q} - \hat{p}^2 \hat{q}}, \tag{7.14a}$$

$$\hat{q}^{w+4} = -\frac{d^2 \hat{p}^2 \hat{q} + d^2 \hat{p} \hat{q}^2 + d^2 \hat{q} - 2d\hat{p} - \hat{p}}{d^2 \hat{p}^2 \hat{q} - 2d\hat{p} \hat{q}^2 + d^2 \hat{p} + d^2 \hat{q} - \hat{p} \hat{q}^2}. \tag{7.14b}$$

This leads to

$$\hat{p} = \frac{1}{d} \left(1 + \frac{\pi^2 d}{2(1+d)} w^{-2} + \frac{2\pi^2 d(d-2)}{(1-d)(1+d)} w^{-3} \right.$$
$$\left. + \left(\frac{\pi^4 d(5d^2+d-1)}{24(1+d)^3} + \frac{6\pi^2(d-2)^2}{(1-d)^2(1+d)} \right) w^{-4} + O(w^{-5}) \right), \quad (7.15a)$$

$$\hat{q} = \exp\left(\pi i \left(w^{-1} + \frac{2(d-2)}{1-d} w^{-2} + \frac{4(d-2)^2}{(1-d)^2} w^{-3} \right.\right.$$
$$\left.\left. - \left(\frac{\pi^2 d(2d^2-5d-1)}{3(1+d)(1-d)^3} + \frac{8(d-2)^2}{(1-d)^3} \right) w^{-4} + O(w^{-5}) \right) \right). \quad (7.15b)$$

The p^w term in the original zero-equations does contribute to the asymptotics of these zeros, however its contribution is exponentially small compared to the above. Consequently,

$$z_c = \frac{d}{(1+d)^2} \left(1 + \frac{\pi^2 d}{2(1+d)} w^{-2} + \frac{2\pi^2 d(d-2)}{(1-d)(1+d)} w^{-3} \right.$$
$$\left. + \left(\frac{\pi^4 d(5d^2+d-1)}{24(1+d)^3} + \frac{6\pi^2(d-2)^2}{(1-d)^2(1+d)} \right) w^{-4} + O(w^{-5}) \right). \quad (7.16)$$

In the limit as $c \to \infty$ (and so $d \to \infty$) we recover the asymptotics of a single non-interacting walk in the strip (see [7]). Observe that if we compensate for the added energy for bound vertices we have

$$\lim_{d \to \infty} \left(z_c \cdot \frac{(1+d)^2}{d} \right) = 1 + \frac{\pi^2}{2} w^{-2} + 2\pi^2 w^{-3} + \left(\frac{5\pi^4}{24} + 6\pi^2 \right) w^{-4} + \cdots,$$

which compares with the similar quantity (from [7]) for a single walk in the strip:

$$2z_c = \frac{1}{\cos(\pi/(w+2))} = 1 + \frac{\pi^2}{2} w^{-2} + 2\pi^2 w^{-3} + \left(\frac{5\pi^4}{24} + 6\pi^2 \right) w^{-4} + \cdots.$$

8 Forces

The asymptotic expressions for the dominant singularity allow us to compute an effective force exerted by the zipping polymer on the confining walls. We define the force (as per the definition in [7]) to be the difference of free energies:

$$\mathcal{F}(c; w) = \frac{1}{2} \left[\log z_c(c; w) - \log z_c(c; w + 2) \right]. \tag{8.1}$$

Substituting in our asymptotic expansions of z_c gives us

$$w^3 \mathcal{F}(c; w) = \begin{cases} 5\pi^2 - \frac{15\pi^2(12 - 7c)}{4 - 3c} w^{-1} + O(w^{-2}) & c < \frac{4}{3} \\ 2\pi - \frac{39\pi^2}{2} w^{-1} + O(w^{-2}) & c = \frac{4}{3} \\ \frac{\pi^2 \sqrt{c(c-1)}}{c} - \frac{3\pi^2 \left(2c(1-c) + (11c - 16)\sqrt{c(c-1)} \right)}{c(3c - 4)} w^{-1} + O(w^{-2}) & c > \frac{4}{3}. \end{cases} \tag{8.2}$$

For a compact expression, we also write the large c result in terms of d:

$$w^3 \mathcal{F}(c; w) = \frac{\pi^2 d}{1 + d} - \frac{3\pi^2 d(3d - 5)}{(d - 1)(d + 1)} w^{-1} + O(w^{-2}) \qquad \text{when } d > 1. \tag{8.3}$$

Note that the leading term is a monotonically increasing function of d (and so c), whose value close to $d = 1$ is $\pi^2/2$ which, we note, is smaller than the value at $c \leq 4/3$. Hence, for sufficiently large w, the force is not monotonic over the whole range $c \geq 1$ and approaches its minimum as $c \to 4/3^+$. This is clearly observable in the plots below. This effect is a result of the competition between entropic and energetic contributions to the force in the different regimes.

We have plotted the above function (8.3) against c for $w = 128$ (up to an including the order w^{-1} terms) along with numerical estimates of $w^3 \mathcal{F}(c; w)$ for $w = 32, 64, 128$ computed via transfer matrices (by comparison of the eigenvalues at widths w and $w + 2$). See Figure 12. To see the small c and large c behaviour more clearly, we also plot the functions restricted to the ranges $[0, 4/3]$ and $[4/3, 10]$ in Figure 13 and 14. Observe that there is excellent agreement between our analytic and numerical results excepting close to the critical value of c — as one might expect. We can also compare our numerical and analytic results exactly at $c = 4/3$ and this is shown in Figure 15
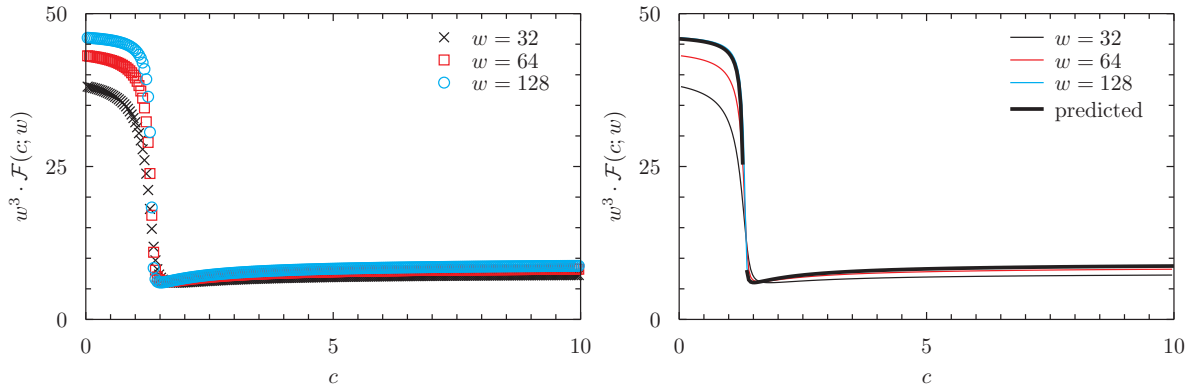
Figure 12: Numerical estimates of $w^3\mathcal{F}$ for $w = 32, 64, 128$ computed using transfer matrices (left) and compared to our predicted result for $w = 128$ (right).
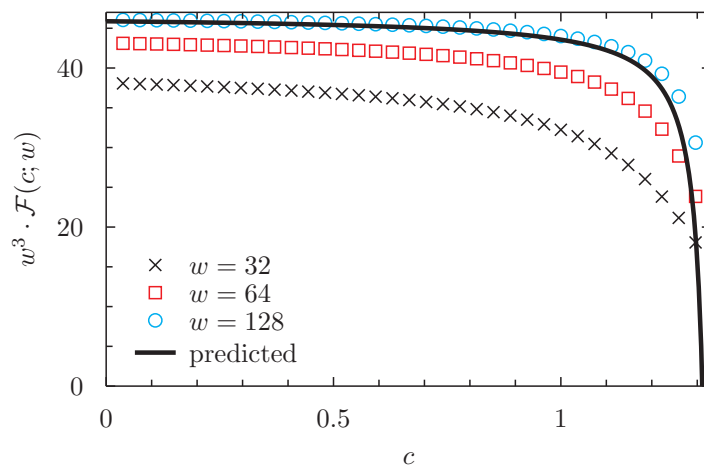

Figure 13: The region $c < 4/3$ for the numerical estimates of $w^3\mathcal{F}$ compared to our predicted result for $w = 128$.

9   Summary

A model of two polymers that can bind together such as DNA confined to be in a long mesoscopic sized strip with parallel walls has been modelled by a directed walk system on the square lattice. We have analysed this model exactly and demonstrated that the force exerted by the polymers provides a signature of the unzipping or denaturation transition seen in the bulk limit. It will be interesting to analyse a system in which there are interactions with the surface as well as inter-polymer interactions such as found in [24] for one wall.
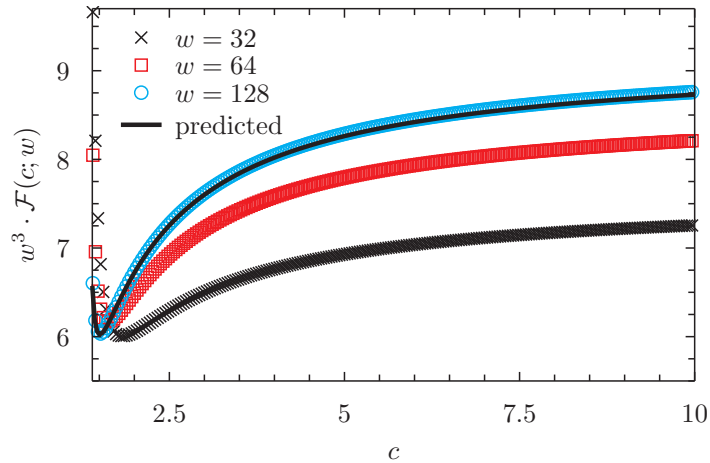
Figure 14: The region $c > 4/3$ for the numerical estimates of $w^3 \mathcal{F}$ compared to our predicted result for $w = 128$.
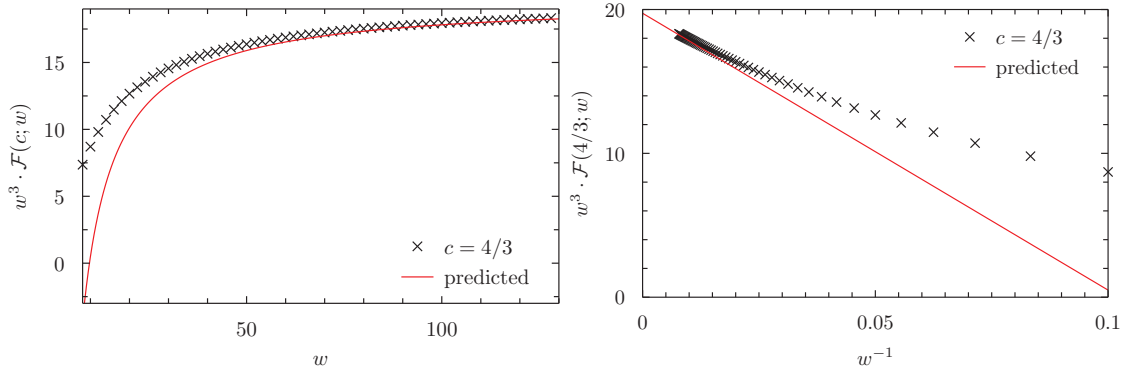

Figure 15: At $c = 4/3$ we compare our predicted asymptotic result with the transfer matrix numerics as a function of w (left) and w^{-1} (right).

Acknowledgements

References

[1] V. Privman, G. Forgacs, and H. L. Frisch, Phys. Rev. B **37**, 9897 (1988).

[2] K. DeBell and T. Lookman, Rev. Mod. Phys. **65**, 87 (1993).

[3] E. J. Janse van Rensburg, *The Statistical Mechanics of Interacting Walks, Polygons, Animals and Vesicles*, Oxford University Press, Oxford, 2000.

[4] A. Rosa, D. Marenduzzo, A. Maritan, and F. Seno, Phys. Rev. E. **67**, 041802 (2003).

[5] E. Orlandini, M. Tesi, and S. Whittington, J. Phys. A: Math. Gen. **37**, 1535 (2004).

[6] J. Krawczyk, A. L. Owczarek, T. Prellberg, and A. Rechnitzer, J. Stat. Mech.: Theor. Exp. , P10004 (2004).

[7] R. Brak, A. L. Owczarek, A. Rechnitzer, and S. Whittington, J. Phys. A **38**, 4309 (2005).

[8] P. K. Mishra, S. Kumar, and Y. Singh, Europhys. Lett. **69**, 102 (2005).

[9] E. J. Janse van Rensburg, E. Orlandini, A. L. Owczarek, A. Rechnitzer, and S. Whittington, J. Phys. A **38**, L823 (2005).

[10] R. Martin, E. Orlandini, A. L. Owczarek, A. Rechnitzer, and S. Whittington, J. Phys. A **40**, 7509 (2007).

[11] K. Svoboda and S. M. Block, Ann. Rev. Biophys. Biomol. Struct. **23**, 247 (1994).

[12] A. Ashkin, Proc. Natl. Acad. Sci. USA **94**, 4853 (1997).

[13] T. Strick, J.-F. Allemand, V. Croquette, and D. Bensimon, Phys. Today **54**, 46 (2001).

[14] B. Essevaz-Roulet, U. Bockelmann, and F. Heslot, Proc. Natl. Acad. Sci. USA **94**, 11935 (1997).

[15] D. K. Lubensky and D. R. Nelson, Phys. Rev. Lett. **85**, 1572 (2002).

[16] D. K. Lubensky and D. R. Nelson, Phys. Rev. E **65**, 031917 (2002).

[17] E. Orlandini, S. M. Bhattacharjee, D. Marenduzzo, A. Maritan, and F. Seno, J. Phys. A: Math. Gen. **34**, L751 (2001).

[18] D. Marenduzzo, S. M. Bhattacharjee, A. Maritan, E. Orlandini, and F. Seno, Phys. Rev. Lett. **88**, 028102 (2002).

[19] D. Marenduzzo, A. Maritan, A. Rosa, and F. Seno, Phys. Rev. Lett. **90**, 088301 (2003).

[20] D. Marenduzzo, A. Maritan, A. Rosa, and F. Seno, J. Stat.Mech. , L04001 (2009).

[21] R.Hegger and P. Grassberger, J. Phys. A. **27**, 4069 (1994).

[22] E. J. Janse van Rensburg and A. Rechnitzer, J. Phys. A **37**, 13869 (2004).

[23] A. Owczarek, A. Rechnitzer, and T. Wong, J. Phys. A: Math. Theor. **45**, 425003 (23pp) (2012).

[24] R. Tabbara, A. L. Owczarek, and A. Rechnitzer, J. Phys. A: Math. Theor. **47**, 015202 (34pp) (2014).

[25] R. Tabbara, A. L. Owczarek, and A. Rechnitzer, J. Phys. A: Math. Theor. **49**, 154004 (27pp) (2016).

[26] R. Brak, G. K. Iliev, A. Rechnitzer, and S. G. Whittington, J. Phys. A: Math. and Theor. **40**, 4415 (2007).

[27] A. L. Owczarek, T. Prellberg, and A. Rechnitzer, J. Phys. A.: Math. Theor. **41**, 035002:1 (2008).

[28] J. Alvarez, E. J. van Rensburg, C. Soteros, and S. Whittington, J. Phys. A: Math. and Theor. **41**, 185004 (2008).

[29] A. J. Guttmann and I. Jensen, Effect of confinement: polygons in strips, slabs and rectangles, in *Polygons, Polyominoes and Polycubes*, pages 235–246, Springer, 2009.

[30] T. Wong, A. Owczarek, and A. Rechnitzer, J. Phys. A: Math. Theor. **47**, 415002 (37pp) (2014).

[31] L. D. Landau and E. M. Lifshitz, *Statistical Physics I*, chapter 1, Pergamon Press, 1980.

[32] P. Flajolet and R. Sedgewick, *Analytic Combinatorics*, Cambridge University Press, 2009.

[33] M. Bousquet-Mélou, Mathematics and Computer Science **2**, 49 (2002).

[34] M. Bousquet-Melou, Discrete Mathematics & Theoretical Computer Science **12**, 65 (2010).